DOI: 10.1021/ma1004106

Macromolecules
ARTICLE

Sphere-to-Wormlike Network Transition of Block Copolymer Micelles Containing CdSe Quantum Dots in the Corona

Meng Zhang,[†] Mingfeng Wang,[†] Shu He,[†] Jieshu Qian,[†] Amir Saffari,[‡] Anna Lee,[†] Sandeep Kumar,[†] Yasser Hassan,[†] Axel Guenther,*[,‡] Gregory Scholes,*[,†] and Mitchell A. Winnik*[,†]

[†]*Department of Chemistry, University of Toronto, 80 St. George Street, Toronto, M5S 3H6 Ontario, Canada, and* [‡]*Department of Mechanical and Industrial Engineering, University of Toronto, 5 King's College Road, Toronto, M5S 3G8 Ontario, Canada*

Received February 20, 2010; Revised Manuscript Received April 20, 2010

ABSTRACT: Poly(styrene-*b*-4-vinylpyridine) (PS_{404}-*b*-$P4VP_{76}$, where the subscripts refer to the number-averaged degree of polymerization) forms spherical crew-cut micelles with a PS core and a P4VP corona when 2-propanol is added to a solution of the polymer in chloroform. When the $CHCl_3$ solution also contains CdSe quantum dots, hybrid micelles form with the QDs bound to the corona. Here we report that vigorous magnetic stirring of a solution of these hybrid micelles in a solution containing 73 vol % 2-propanol leads to a morphology transformation to form three-dimensional wormlike networks that have structural features similar to that first reported by Jain and Bates [*Science* **2003**, *300*, 460−464] for a poly(butadiene-*b*-ethylene oxide) block copolymer in water. Under the influence of shear, PS_{404}-*b*-$P4VP_{76}$ micelles appear to aggregate and then rearrange to form colloidally stable networks consisting of wormlike micelles, uniform in width, that are present as loops and tails connected by T- and Y-junctions. The wormlike micelles are similar in width to the original hybrid micelles, whereas the tails of the micelles have thicker bulbous end-caps. This morphology transition is extremely sensitive to solvent composition and is also affected by the stirring rate.

Introduction

Amphiphilic block copolymers self-assemble into micelle-like objects when dissolved in solvents that are selective good solvents for one of the blocks.[1] Most diblock copolymers form spherical micelles in selective solvents, particularly those with long soluble chains and short insoluble core-forming chains. "Crew-cut" micelles are formed when the soluble, corona-forming chains are shorter than the characteristic size of the core formed by the insoluble block. A variety of different morphologies can form for these types of polymers.[2,3] Examples include spherical micelles, raftlike planar structures,[4] bilayers,[5,6] and cylinders.[7−10]One of the attractive features of these structures is that micelle morphology can often be tuned by tailoring (1) the nature of the block copolymer, such as the chemical composition, architecture, the length of each block, and the polydispersity, and (2) the nature of the host medium, such as the choice of solvent, pH, ionic strength, and concentration of block copolymer. As a consequence, block copolymers have a broad range of current or potential applications in materials science[11−13] and biomedical engineering.[14−17] Block copolymer micelles can serve as structural components, for example, as toughening agents for epoxy resins, as carriers of drugs or dyes for biomedical applications, or as robust scaffolds for the co-organization of functional polymers, inorganic nanocrystals, and organic dyes at the nanoscale.

Very recently, a number of reports have appeared in the literature describing examples in which processing conditions have led to a change in block copolymer micelle morphology. Larue et al.[18] described a reversible transition from cylindrical poly(styrene-*b*-isoprene) (PS−PI) micelles in hexane to spherical micelles as the solution temperature was raised from 25 to 35 °C. The authors showed that this transformation operated under thermodynamic control, in which the increase in temperature led to increased swelling of the core by the solvent. In other examples, factors other than thermodynamics play a key role. For example, Wu's group[19] in China reported that extrusion of a solution of PS−PI crew-cut micelles in a mixture of *n*-hexane and THF through a uniform nanoporous membrane with pore sizes smaller than the micelle diameter transformed the objects into elongated cylindrical micelles. Upon standing, the micelles eventually broke up to re-form the spherical micelles. Yu and Jiang[20] examined the influence of shear on the morphology of micelles formed by (4-vinylpyridine-*b*-styrene-*b*-4-vinylpyridine) (P4VP−PS−P4VP) triblock copolymer micelles in a dioxane−water mixture. This polymer formed long (several micrometers) cylindrical micelles as prepared in solution. When subjected to shear by intense stirring, the objects broke up to form some shorter rods but also cyclic (toroidal) structures, both with contour lengths less than 500 nm. Other examples have been reported where a change in temperature[21] or in micelle formation conditions[22] led to elongated structures.

We are interested in block copolymer micelle−inorganic nanocrystals hybrid composite structures. The idea of this research is to use the structure of the micelle as a motif for organizing the location of nanocrystals such as quantum dots (QDs). QDs are important nanomaterials for applications in light-emitting diodes,[23] biosensors,[24] and photovoltaic cells[25] due to their broad continuous absorption and narrow, size-dependent emission at high quantum yield.[26] In a previous publication,[27] we described the preparation of spherical crew-cut PS−P4VP block copolymer hybrid micelles with CdSe QDs bound to the corona adjacent to the core, with a conjugated polymer (poly(3-hexylthiophene), P3HT) confined to the PS core. Upon photoexcitation of the

*Corresponding authors. E-mail: axel.guenther@utoronto.ca (A.G.); gscholes@chem.utoronto.ca (G.S.); mwinnik@chem.utoronto.ca (M.A.W.).

 Published on Web 05/13/2010

QDs, the presence of the P3HT led to the quenching of the QD photoluminescence due to energy transfer or charge transfer across the core−corona interface as a heterojunction. We envisioned this type of structure as a very simple nanoscale light harvesting system in which the QDs serve as the antennae that absorb light and transfer energy to the conjugated polymer in the micelle core.

We have been trying to build analogous structures elongated in shape, starting originally with the idea that we could use block copolymers that formed cylindrical micelles as the organizing motif. While considering ways to meet this goal by changing polymer composition, chain length, or solvent composition, we made a remarkable observation: that stirring solutions of the same PS−P4VP block copolymer and CdSe QD samples, in a mixture of chloroform and 2-propanol (2-PrOH), led to a morphology transformation. Because of the presence of the QDs, the micelles aggregated to form wormlike structures (with diameters similar to that of the spherical micelle precursors) that looped or intersected at T- or Y-junctions to form finite-sized but colloidally stable aggregates. In this paper we describe the results of experiments designed to explore this aggregation phenomenon.

Experimental Section

Materials and Methods. The diblock copolymer PS_{404}-*b*-$P4VP_{76}$ (M_n = 50 100, M_w/M_n = 1.08, where the subscripts indicate the number of average degrees of polymerization) was purchased from Polymer Source Inc. Dorval, Quebec, Canada. A stock solution of this polymer (1.0 mg/mL) in chloroform was used for preparing micelles.

Trioctylphosphine oxide (TOPO)-coated CdSe(555) QDs were prepared by the traditional organometallic approach at high temperature in the presence of trioctylphosphine oxide (TOPO).[28] The number in parentheses (555) refers to their band edge absorbance maximum in nanometers. Excess TOPO ligands were removed by three successive cycles of precipitation in methanol followed by redispersion in $CHCl_3$. The concentration of CdSe/TOPO was estimated through the Beer−Lambert law ($c = A/\varepsilon L$), where the extinction coefficient (ε) of CdSe QDs was determined by the empirical equation $\varepsilon = 5857d^{2.65}$ (d is the diameter of CdSe QDs measured by TEM).[29] The CdSe/TOPO QDs we employed had a mean diameter of 2.7 ± 0.5 nm as measured by TEM. The CdSe/TOPO nanorod sample, with a band-edge absorbance at 555 nm, was prepared as described in the literature.[30] The concentration of CdSe nanorods in $CHCl_3$ was determined by weight.

Preparation of the Micelles. The sample solutions were prepared by premixing 1 mL aliquots of a PS_{404}-*b*-$P4VP_{76}$ chloroform solution (1.0 mg/mL) with 0.25 mL samples of CdSe(555)/TOPO in $CHCl_3$ (2.5 mg/mL) in 20 mL screw-capped scintillation vials. The QD−polymer ratio was fixed at 0.6 mg of QD per mg of diblock copolymer. To promote mixing, the mixture was stirred for 30 min with a Teflon-coated magnetic bar (1.3 cm × 0.4 cm) at room temperature before the addition a selective solvent, 2-propanol (2-PrOH). Later experiments showed that stirring for only a few minutes before addition of 2-PrOH gave similar results. For most solutions, the volume fraction of 2-PrOH (φ_{2PrOH}) was 0.73 ($CHCl_3$/2-PrOH, 3:8, v/v). To examine the effect of prolonged stirring on the micelle morphology, the samples were sealed in the vials by wrapping the threads with Teflon tape before the cap was attached. Then the top of the capped vial was wrapped with parafilm. These solutions were then stirred at various rates, primarily 1250 rpm. Small aliquots were taken periodically (e.g., at 6, 12, 24, and 50 h) for examination by TEM. Some samples were stirred in this way for 5 days.

Transmission Electron Microscopy (TEM). Transmission electron microscopy (TEM) measurements were performed on a Hitachi HD2000 STEM microscope operating at an accelerating voltage of 200 kV and with a Hitachi a D-7000 CTEM microscope operating at an accelerating voltage of 100 kV. In the dark-field mode, electron-dense objects appear bright, whereas electron-dense objects appear dark in the bright-field mode. The samples were prepared by depositing one drop of sample solution onto a 300 mesh copper grid coated with a carbon-stabilized Formvar film. The excess sample solution was absorbed by a filter paper placed beneath the copper grid, and the solvent was allowed to evaporate in the ambient environment. TEM images were analyzed using Image J, an image processing program developed at the National Institutes of Health.

Turbidity Measurements. Optical absorption spectra were measured at room temperature on a Perkin-Elmer Lambda 25 spectrometer using 1.00 cm quartz cuvettes. We characterize the sample's turbidity by monitoring the optical absorption at 650 nm where the samples have no absorbance.

Dynamic Light Scattering. Right-angle dynamic light scattering (DLS) measurements were carried out at 25.0 ± 0.05 °C using an instrument from ALV described previously.[31] Size information was obtained by analysis of the autocorrelation function decay by CONTIN,[32] using software included with the ALV instrument.

Results and Discussion

The amphiphilic diblock copolymer PS_{404}-*b*-$P4VP_{76}$ has a long PS block and a relatively short P4VP block, which can serve as multidentate ligand for binding semiconducting nanocrystals, such as the QDs examined here.[33,34] In a previous publication,[27] we showed that solutions of this polymer plus very similar CdSe QDs (CdSe(559), 100 μg/mg PS−P4VP) in $CHCl_3$ self-assembled into "crew-cut" spherical micelles when various alcohols (*n*-butanol, 2-PrOH, and methanol) were added. $CHCl_3$ is a common good solvent for both polymer blocks and for the QDs, whereas the alcohols are precipitants for PS and for TOPO-coated QDs. These micelles persisted when the $CHCl_3$ was removed by evaporation, and most of the attention in that paper was on the properties of the hybrid structures in chloroform-free alcohol solutions. Here we focus on the micelle properties in solvent mixtures of $CHCl_3$ and 2-PrOH. The diblock copolymer solution in $CHCl_3$ was mixed with solutions of the CdSe(555) QDs in $CHCl_3$ (0.18 mg/mL polymer, 0.6 mg of QD per mg of polymer), and then the appropriate amount of 2-PrOH was added. Most solutions had a solvent composition of φ_{2PrOH} = 0.73. Aliquots examined by transmission election microscopy (TEM) showed the presence of hybrid micelles as shown in Figure 1A. The average diameter of the spherical micelles measured in the TEM images was 38 ± 4 nm. These micelles contained QDs (the tiny bright dots in dark-field TEM image) in the P4VP corona. These solutions were transparent to the eye, as shown in the digital photograph in the inset to Figure 1A.

On close inspection of many TEM images, we found no free QDs and very few micelles bearing no QDs. In most areas of the TEM grid, isolated micelles were observed. However, in some regions on the TEM grid surface, we found pairs of adjacent micelles or occasionally groups of three micelles. We did not have enough of this CdSe(555) QD sample for dynamic light scattering (DLS) studies. In our previous study of the same polymer plus CdSe(559) QDs, after the removal of chloroform,[27] we found similar small numbers of small micelle aggregates in TEM images. DLS studies of those micelles showed no evidence for any micelle aggregates in solution. Thus, we concluded that these micelle pairs and triads formed during solvent evaporation on the grid. To test whether these kinds of aggregates are present in solution here, we carried out DLS measurements on similar micelles formed from the same PS−P4VP and a new batch of QDs of a somewhat different size (CdSe(540)/TOPO). These results are presented in Figure S1 in the Supporting Information.

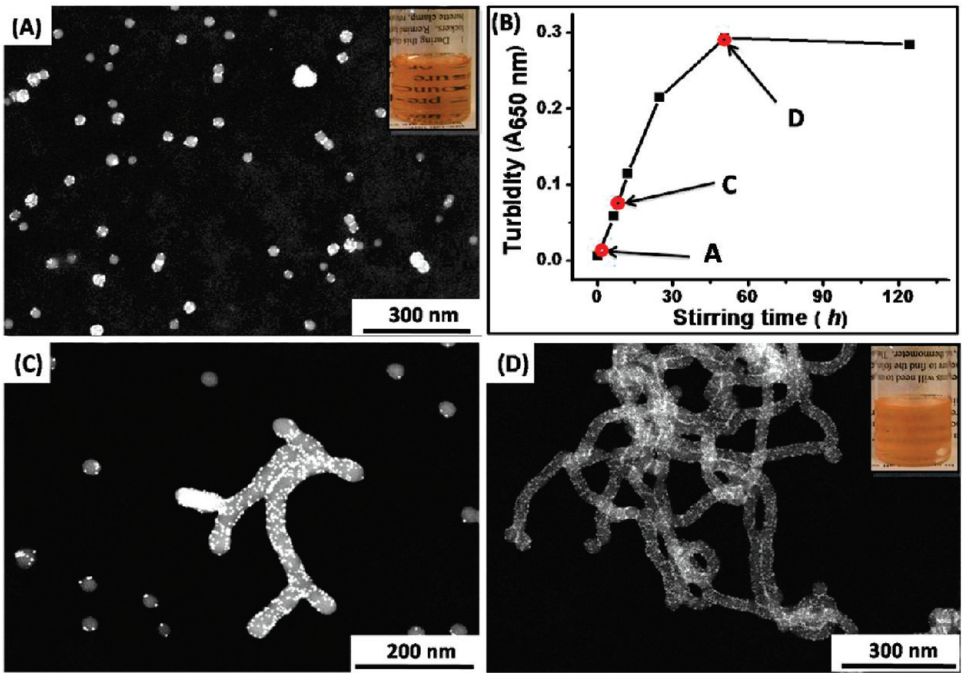

Figure 1. Turbidity measurement (B) monitored the morphology evolution of PS_{404}−$P4VP_{76}$/CdSe(555) micelles in $CHCl_3$/2-PrOH ($\phi_{2\text{-PrOH}} = 0.73$, $\phi_{2\text{-PrOH}}$ is the volume fraction of 2-PrOH) as a function of stirring time. At different stirring times (indicated as red circles), dark-field TEM images were taken to present the morphology transition from (A, 5 min) spheres to (C, 6 h) coexistance of sphere and wormlike micelle to (D, 50 h) wormlike networks. Inset (A, D): digital photos of the sample taken at corresponding stirring time.

They show that hybrid micelles were present with an apparent hydrodynamic radius of 15 nm and a narrow size distribution. These experiments confirm the conclusion that the initially prepared hybrid micelles are free of aggregates and that the small aggregates seen on the TEM grid are formed as the sample dried. These DLS experiments also show the presence of aggregates after prolonged stirring (Figure S1).

When this block copolymer−QD hybrid micelle solution was allowed to age for 30 h without stirring, we found a solid red precipitate at the bottom of the vial. At the same time, the solution above the precipitate remained transparent, but the color had faded slightly. A dark-field TEM image (Supporting Information, Figure S2) of this solution showed that it consisted of many small aggregates and a much smaller number of individual hybrid micelles. We were not able to redisperse the precipitate by vigorous stirring.

In contrast, when a freshly prepared solution of the same composition was stirred vigorously (via a Teflon-coated magnetic bar, 1250 rpm), the solution gradually turned cloudy but remained colloidally stable. Sample turbidity was monitored at 650 nm, a wavelength where the components have no absorbance. The turbidity increased over a period of hours, leveling off after about 50 h (Figure 1B). The increase in turbidity was a consequence of the formation of aggregates in the system large enough to scatter light. Another striking feature of these samples was that these turbid QD−polymer hybrid solutions showed surprisingly good colloidally stability. For instance, we allowed a sample solution stirred for 50 h at 1250 rpm to age without stirring for 3 months. While the contents settled as fluffy aggregates on the bottom of the vial due to the high density of QD−polymer hybrids, they were readily redispersed. They formed a uniform turbid solution after a few seconds of gentle shaking. TEM measurements showed no significant changes in the morphology of the aggregates present. The nature of these aggregates is described in more detail in the following section. One of the unfortunate consequences of prolonged vigorous stirring in the presence of air was a strong decrease in the photoluminescence intensity of the CdSe QDs in the hybrid structures. This is likely a consequence of surface oxidation leading to the formation of traps on the surface of the QDs.

Evolution of CdSe(555)/PS_{404}−$P4VP_{76}$ Micelles from Spheres to Wormlike Networks. Aliquots were removed from the stirred solutions of the PS_{404}-*b*-$P4VP_{76}$/CdSe(555) hybrid micelles in $CHCl_3$/2-PrOH and placed on carbon-stabilized Formvar-coated copper grids for examination by transmission (TEM) and scanning (SEM) electron microscopy. For the sample stirred 6 h, we found individual spherical micelles in combination with extended wormlike structures. A dark field TEM image of one such structure is presented in Figure 1C. These average widths of the wormlike micelles were comparable to the diameter of free spherical micelles, whereas enlarged semispherical end-caps terminated both ends of the wormlike micelles. In addition, some "bud"-like objects were attached to the body of the structure. The sample solution was cloudy.

When the stirring time reached 50 h, the turbidity of diblock copolymer/QD hybrids became constant. The sample solution became very cloudy as shown in the inset of Figure 1D. An aliquot was removed for analysis by electron microscopy. One image is presented in Figure 1D. A collection of representative TEM and SEM images of the structures present on the microscopy grid is presented in Figure 2. These images show that vigorous stirring promoted the aggregation of the QD−polymer hybrid micelles into finite-sized networks. The structures of these networks have features in common with those described by Jain and Bates[8,35] for a poly(butadiene-*b*-ethylene oxide) (PB-*b*-PEO) diblock copolymer in water. We reproduce two examples from the work of Jain and Bates in Figure 2H,I and use their language to describe characteristic features of the network structure. We note that similar network structures have been reported for a poly(styrene-*b*-ethylene oxide) (PS−PEO) diblock copolymer in *N,N*-dimethylformamide−acetonitrile mixtures.[36]

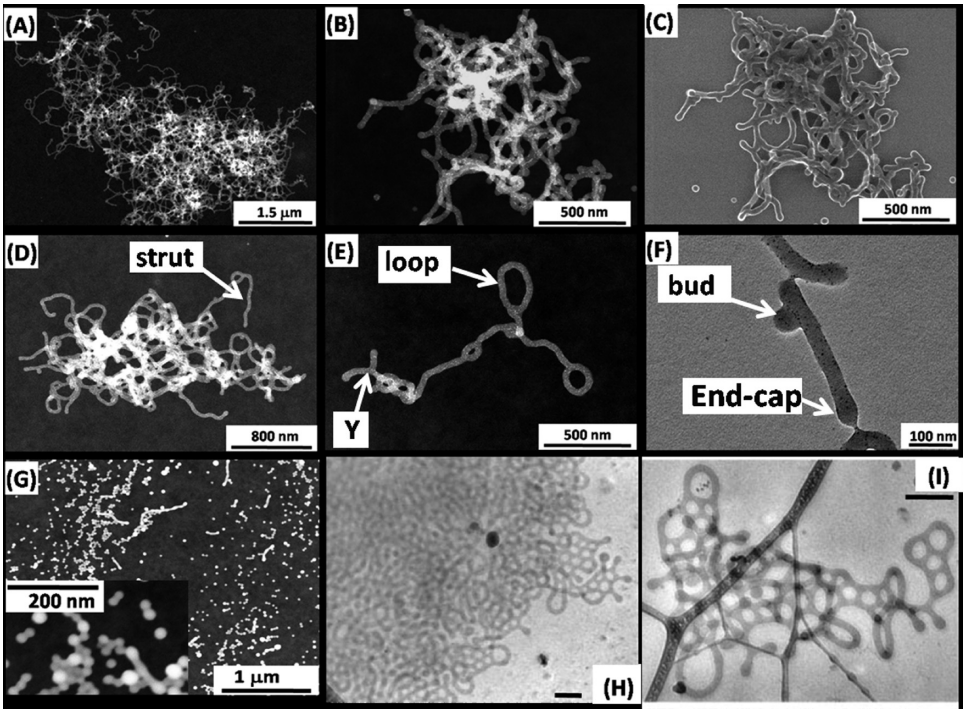

Figure 2. Dark-field TEM images (A, B, D, E) and an SEM image (C) of wormlike networks formed by CdSe(555)/PS_{404}-*b*-$P4VP_{76}$ hybrid micelles after stirring a solution in 2-PrOH/$CHCl_3$ ($\phi_{2\text{-PrOH}} = 0.73$) at 1250 rpm for 50 h. A high-magnification image (F) is provided under bright-field mode. (G) Dark-field TEM image of PS_{404}−$P4VP_{76}$ micelles in the absence of quantum dots in $CHCl_3$/2-PrOH ($\phi_{2\text{-PrOH}} = 0.73$) after stirring for 50 h (a higher magnification image is in the inset). For comparison, from ref 8, cryo-TEM images (H, I) of aqueous dispersions of a network containing loops and Y-junctions formed by a PB-*b*-PEO sample with $w_{PEO} = 0.34$. A smaller network fragment (I) is provided with more morphology details, scale bars (H, I), 200 nm. (H, I) are reproduced with permission from ref 8. Representative structural elements are indentified in several of the panels of the figure: worm-like strut in (D), loop and Y-junction in (E), bud and end-cap in (F).

The TEM and SEM images presented in Figure 2 show that the polymer/QD network structures consist of the following four building blocks: (1) T- or Y- junctions, (2) loops, (3) wormlike struts connecting the T-/Y-junctions, and (4) "buds" or "end-caps". Wormlike loops in the interior of the network contained two or more T-/Y-junctions, whereas some loops were attached to the more linear framework via a single junction. The budlike protrusions appeared to be attached randomly along the wormlike struts or loops. Very few isolated spherical micelles could be seen in these images.

There are some important differences between the structures we observe and those reported by Jain and Bates. They used cryo-TEM to study the self-assembly of a series of PB-*b*-PEO diblock copolymers in aqueous solution and found network structures for samples with a weight fraction of PEO (w_{PEO}) ≈ 0.34 and a sufficiently long PB block. The structures they described appear two-dimensional. The authors proposed that this is the consequence of thickness confinement when preparing thin vitrified films of sample solution for cryo-TEM analysis. In contrast, the networks formed in our case appear to be three-dimensional objects that collapse on the grid during drying. This idea is supported by comparing the dark-field TEM image in Figure 2B with the SEM image of the same object in Figure 2C. In the SEM image, one can see that the object is thinner at the edges, and there is evidence for the layering of parts of the network closer to the center of the object. There is also a difference in the symmetry of the network structures. The images in the Jain and Bates papers often showed mirror symmetry, which the authors attributed the redistribution of the macromolecules (PB-*b*-PEO) within the micelles to minimize their surface free energy to achieve the local near-equilibrium structures. This unhindered movement was a consequence of the low glass transition temperature (T_g, ca. −12 °C) of the PB block. We do not see any evidence for symmetry in the electron microscopy images of PS−P4VP/QD hybrid networks formed through stirring, although it is possible that symmetry in the structures could be masked when the networks collapse on the grid. We do, however, see a broad distribution of network sizes, ranging from hundreds of nanometers to micrometers in the longest dimension.

A control experiment was carried out to see if the presence of the QDs was necessary for micelle aggregation upon stirring and formation of the networks. A sample of the PS-*b*-P4VP diblock copolymer solution in $CHCl_3$/2-PrOH at the same concentration but without QDs was treated as described above. A TEM image taken of a sample after brief stirring (Figure S3, Supporting Information) showed only free spherical micelles. Then this solution was stirred at 1250 rpm for 50 h. An aliquot was taken for TEM analysis, and an image is presented at low magnification in Figure 2G and at higher magnification in the inset to Figure 2G. The sample consists primarily of spherical micelles plus a small number of elongated aggregates. Some of the spherical micelles appear larger than others, and in the elongated structures, the end-caps appear larger than the pearl-like constituents along the backbone. The aggregates look like they were formed by collision of spherical micelles. The larger spherical structures may have been formed by shear-induced collisions of micelles under stirring. No large networks were formed. The QDs appear to be necessary element in the solution for the networks to form.

Influence of QDs on the Morphology of the Hybrid Micelles. One of the curious features of the QD/micelle hybrids formed when 2-PrOH is added to a solution of PS_{404}-*b*-$P4VP_{76}$ + CdSe(555) in $CHCl_3$ is the rather broad distribution of QDs among the micelles. To quantify this distribution, we examined

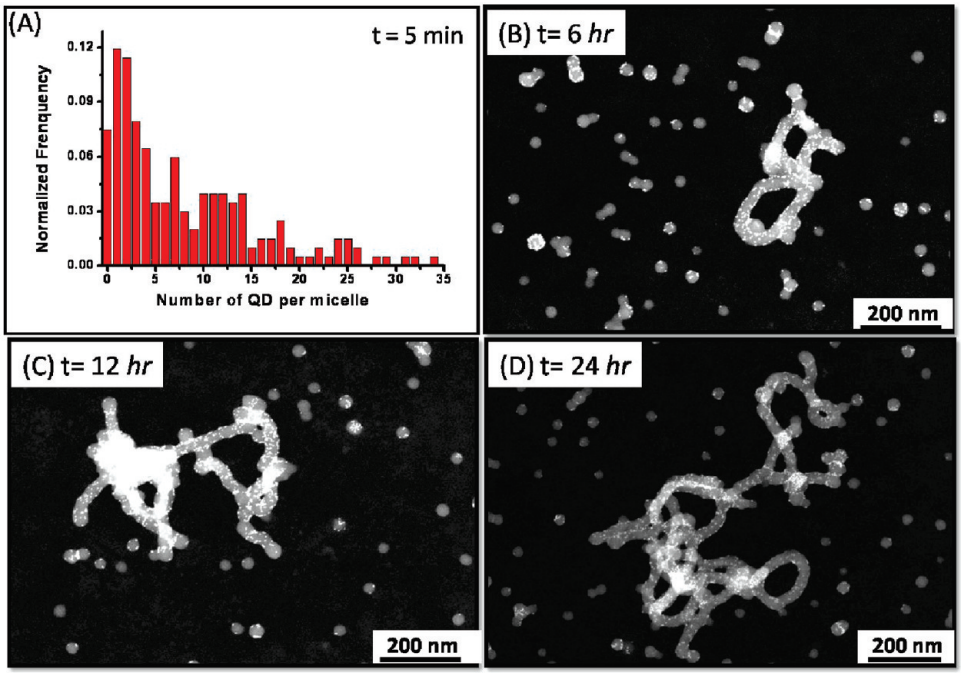

Figure 3. (A) Normalized QD distribution per PS_{404}-*b*-$P4VP_{76}$/CdSe(555) micelle at stirring time of 5 min. The histograms are constructed based on TEM analysis of 200 hybrid micelles. Dark-field TEM image of PS_{404}-*b*-$P4VP_{76}$/CdSe(555) in a $CHCl_3$/2-PrOH ($\phi_{2\text{-PrOH}}$ = 0.73) solution at agitation time of (B) 6 h, (C) 12 h, and (D) 24 h, showing the distribution of the QD per micelle.

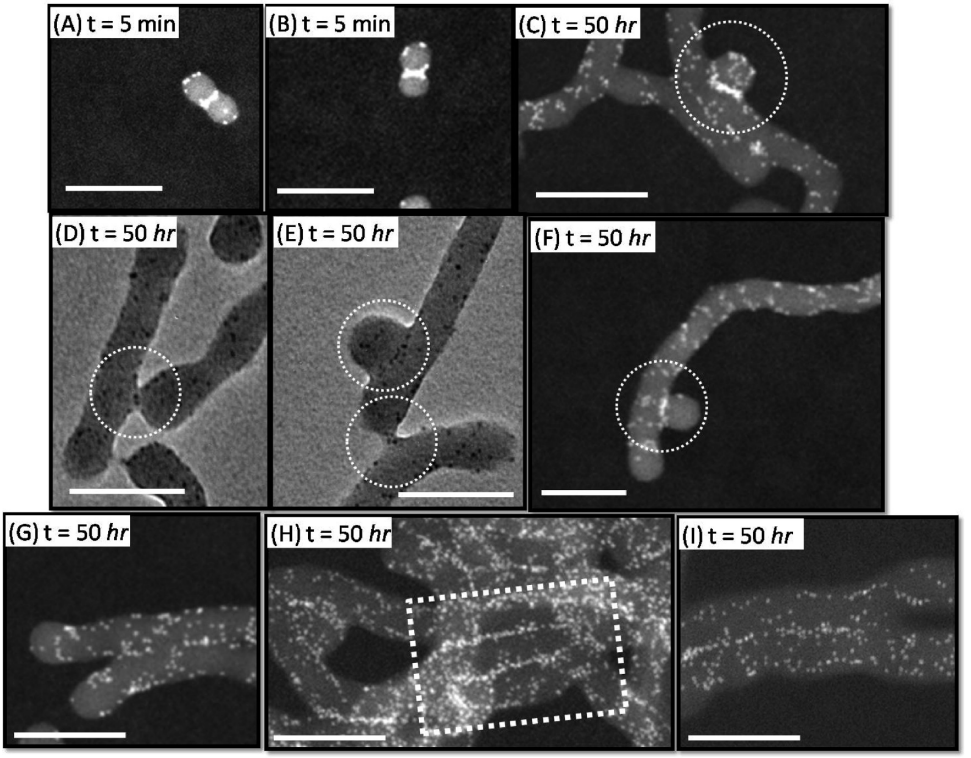

Figure 4. Dark-field TEM images (A−C, F−I) and bright-field TEM images of (D, E) of CdSe QD contained PS-*b*-P4VP network fragments in $CHCl_3$/2-PrOH ($\phi_{2\text{-PrOH}}$ = 0.73) taken at certain agitati on time shown in the inset. The "collision/fusion" interfaces are found between spherical−spherical (A, B), spherical−strut (C, D, E, F), and strut−strut micelles (E, G, H, I). The scale bars are 100 nm in all images.

dark-field TEM images at high magnification from freshly prepared samples. As one can see in Figure 3 (and also in Figure 4), the QDs appear as bright dots and can be counted. A histogram constructed from the analysis of 200 hybrid micelles is presented in Figure 3A. The average number of QD per micelle is about 8, and ca. 90% of the micelles contain fewer than 20 QDs. About 7% of the micelles have no detectable QDs, although we cannot be certain that we could detect QDs attached to the back (grid) side of the micelles.

Figure 3B−D presents images taken from a solution stirred for 6, 12, and 24 h at 1250 rpm. The images are chosen to illustrate one large aggregate and the surrounding

background of isolated spherical micelles. The number of free micelles decreased from the 6 h sample to those stirred for longer times. Recall that after 50 h (e.g., Figure 2) very few free micelles can be found. Here we would like to emphasize that the free micelles that remain, on the whole, contain fewer QDs than those present in the initially prepared solution. We interpret these observations to indicate that micelle aggregation is promoted by micelles that contain the largest number of QDs in their corona.

We next turn our attention to the question of how the presence of the QDs affects the morphology of the block copolymer−QD aggregates. We begin by examining at relatively high magnification (Figure 4A,B) two pairs of doublets found in TEM images of a sample stirred for only 5 min. As discussed above, these are rare objects in the TEM images of this sample. It is possible that these dimers may have formed in solution but more likely that they formed as the solvent evaporated on the grid. The most striking feature of these doublets is the extensive localization of QDs at the junction between the two micelles. In Figure 4A, most but not all of the QDs are found in the interface. In Figure 4B, the effect is even more pronounced, since all of the QDs in the lower micelle are at the junction. The observation of substantial numbers of QDs at the junction between micelles in these dimer aggregates suggests that the QDs promote aggregation by making the surface of the QDs sticky to collisions with other QDs. This idea is supported by the much smaller tendency for aggregation seen in QD-free micelles subjected to stirring (Figure 2G). In our view, it is unlikely that the QDs in individual micelles become localized in patches on the micelle surface prior to interaction with a second micelle.

Figure 4C−I presents TEM images of structures from solutions stirred at 1250 rpm for 50 h. These images emphasize the wormlike nature of the struts present in the network structures. Figure 4C,E shows buds protruding from a wormlike host. The structure in Figure 4C is interesting because it consists in part of two wormlike objects attached in parallel. Figure 4D,E shows other examples, here in bright field, of intersections between elongated objects. Buds are prominent in the structures in Figure 4E,F. In both cases, QDs are concentrated at the junction, whereas in the rest of the structure away from the contact zone, QDs are sparser and randomly distributed. Figure 4G−I presents three examples of parallel wormlike sections that have come into contact. Analysis of these and other images from this sample indicates that the diameters of the buds and end-caps were similar, 49 ± 4 nm, whereas the average diameter of the wormlike strut was 40 ± 5 nm. Histograms of these size distributions are provided in Figure S4 (Supporting Information).

On the basis of these observations, we infer that QDs actively participate in the micelle aggregation process as "bridging agents". The PS−P4VP micelle binds to the TOPO-capped QDs in its corona by replacing many TOPO molecules with 4-VP groups from the polymer. Thus, P4VP acts as a multidentate ligand. In a previous paper,[27] we compared the dry diameter of these hybrid micelles determined by TEM with the hydrodynamic diameter determined by DLS and deduced that the P4VP corona was on the order of only 2 nm thick. QDs bound to this layer at the micelle surface are also close to the exterior edge of the corona. Shear-induced collisions may lead to bridging interactions ("sticky" collisions) in which individual QDs bear 4-VP ligands originating from the P4VP corona of two different micelles. These ideas can explain the formation of dimer structures as in Figure 3A,B as well as the buds attached to the sides of wormlike struts, but it does not explain how the micelles fuse to form elongated wormlike structures. We imagine that in the mixed solvent employed for these experiments ($\varphi_{2PrOH} = 0.73$) there is sufficient chloroform, a good solvent for PS, to plasticize the micelle core. Over time, fusion occurs, leading to a continuous PS phase in the core of the wormlike structure. The absence of large spherical structures, which would have lower surface energy, must be dictated by limits to microphase separation imposed by the chain length and composition of the PS−P4VP block copolymer molecules.

Influence of Shear Rate on the Morphology of CdSe(555)/PS_{404}−$P4VP_{76}$ Micelles. In this section, we explore the influence of stirring rate on the micelle aggregation and morphology evolution processes. Samples with identical compositions to those described above (0.18 mg/mL polymer, 0.6 mg QD/mg polymer, $\phi_{2PrOH} = 0.73$) were prepared and then stirred for 50 h at 250, 750, and 1250 rpm. As shown in Figure S5 (Supporting Information), samples stirred at both 250 and 1250 rpm showed an increase in turbidity with stirring time, eventually leveling off. This figure shows a somewhat higher limiting turbidity for the sample with the slower stirring rate. Representative dark-field TEM images of aggregates formed after 50 h at these different stirring rates are shown in Figure 5. The image in Figure 5A is of a large aggregate with a longest dimension larger than 5 μm. As one can see more clearly in the blowup of a portion of this aggregate in Figure 5B, the internal morphology is similar to that of the aggregates formed at 1250 rpm: wormlike structures decorated with QDs that form loops and dangling ends, connected by T- and Y-junctions. Figure 5C,D provides for comparison images of networks formed at stirring rates of 750 and 1250 rpm. While the internal structure of the networks is not noticeably different from those formed at the slower shear rate, we cannot get sufficient information from TEM images to know if the overall size distribution varies with stirring rate. More significantly, at the slower stirring rates, one can identify larger numbers of free micelles in the TEM images, along with a few wormlike linear objects. Examples of free micelles in the images are indicated by the white arrows in Figure 5.

The most likely explanation for the results described above is that shear promotes sticky collisions, initially between micelles and later between micelles and larger aggregates. Adhesion is promoted by the QDs in the corona of the micelles and followed by fusion of the PS cores. The $CHCl_3$ present in the solvent must plasticize the PS cores and impart enough mobility for the PS chains for this fusion to occur. Extensive fusion is required for extended networks to form. The finite size of the aggregates formed under shear suggests that shear is also responsible for limiting network growth, for example, through degradation of large networks into smaller entities. One anticipates that shear degradation would be most prominent at the highest shear rates.

Quantifying the influence of shear is a daunting task for this type of stirring, since the shear fields within the vial vary as a function of distance from the stirring bar and location in the vial. The images in the insets in Figure 5 show that more rapid stirring creates a deeper vortex within the vial. Perez et al.[37] point out that for this type of stirring the highest values of the shear rate, at the tip of the magnetic stirring bar, could be 50 times above the average shear rate. Soos et al.[38] argue that fracture of aggregates in suspension is controlled by the maximum rather than the mean shear rate. They studied the aggregation of anionic polystyrene latex particles induced by the presence of positively charged aluminum

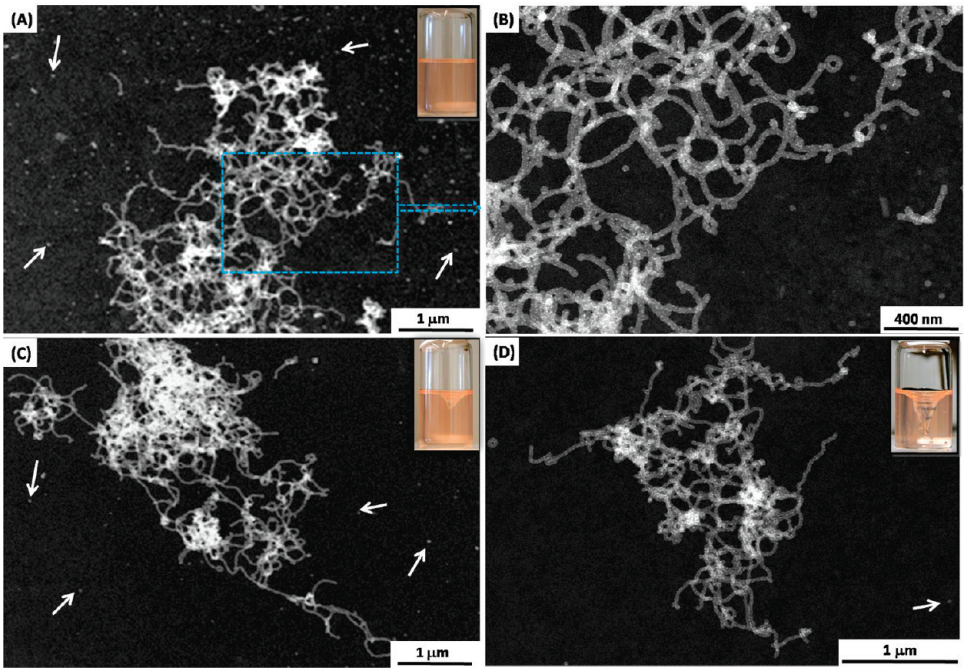

Figure 5. Dark-field TEM images of PS_{404}−$P4VP_{76}$/CdSe(555) stirred at (A) 250 rpm, (C) 750 rpm, and (D) 1250 rpm for 50 h. (B) is the higher magnification TEM image of the selected area in (A). Arrows are pointing to remaining spherical micelles. Digital photos of sample solutions stirred at 250 rpm (A inset), 750 rpm (C inset), and 1250 rpm (D inset).

ions. In their system, the Al(III) ions serve as a "glue" to promote adhesion of PS particles, which has some similarities to the QDs in our system serving as bridges between the corona of adhering micelles. The relatively long times required in our experiments for the morphology to evolve may be caused, at least in part, by the low probability of a fluid element to pass through a maximum shear region. Under these circumstances, employing a sample geometry with a better-defined shear rate would be a promising approach to fabricate networklike micelles in a controllable manner. Experiments to explore this idea are under consideration.

Influence of the Solvent Composition on the Morphology of the Hybrid Micelle Aggregates. One way to manipulate the ability of the solvent to plasticize the PS core of the block copolymer micelles is to vary the solvent composition. In this section, we examine the results of experiments for three different solvent compositions containing different amounts of 2-PrOH (ϕ_{2PrOH} = 0.67, 0.73, and 0.77). These solutions were prepared by adding requisite amounts of 2-PrOH into chloroform solutions of the block copolymer and QDs, keeping the final concentrations of the QDs and polymer constant (0.18 mg/mL polymer, 0.6 mg QD/mg polymer). These sample solutions were stirred at 1250 rpm for 50 h before performing TEM measurements.

Figure 6 shows the morphology of typical aggregates of hybrid QD/PS−P4VP micelles obtained after stirring solutions at different solvent compositions for 50 h at 1250 rpm. Wormlike networks were formed only for solvent compositions close to $\phi_{2\text{-PrOH}}$ = 0.73. For example, at $\phi_{2\text{-PrOH}}$ = 0.67 (Figure 6A) we found networks comprised of bridged spherical micelles that did not fuse into wormlike micelles. At lower alcohol content (e.g., $\phi_{2\text{-PrOH}}$ = 0.65, Figure S6A, Supporting Information) only free spherical micelles were found. On the other hand, when the alcohol content was increased slightly to $\phi_{2\text{-PrOH}}$ = 0.77 (Figure 6C), smaller networks formed that resembled branched wormlike micelles. Typical dimensions were several hundred nanometers in length. These structures were accompanied by large numbers of spherical micelles apparently unchanged by stirring. At higher alcohol content (e.g., $\phi_{2\text{-PrOH}}$ = 1.0; Figure S6B, Supporting Information), the spherical micelles agglomerate into ill-defined aggregates under these stirring conditions. Thus, the formation of wormlike networks is extremely sensitive to solvent composition and takes place within a very narrow window of solvent composition.

With an increase of selective solvent in the solvent mixture, changes occur in the structure of block copolymer micelles. The corona chains become more swollen, and core-forming chains become more closely packed. As a consequence, the packing geometry of the micelles can rearrange to reflect the balance of free energy between the repulsion among swollen corona chains and the extension of core-forming chains. For example, Bhargava et al.[39] established a phase diagram for self-assembled PS_{962}-*b*-PEO_{227} diblock copolymer structures that describes the morphology as a function of dimethylformamide−acetonitrile solvent mixtures. Within a very narrow range of solvent composition (45−50 wt % CH_3CN, a selective solvent for PEO), wormlike networks were formed. Outside this range, wormlike networks coexisted with spheres or vesicles. In the case of the QD/PS−P4VP system described here, the formation of branched networks requires a favorable content of selective solvent to provide the driving force for a transformation to a wormlike morphology. Micelle fusion to form these wormlike micelles also requires a sufficient mobility of the core-forming PS block. When the 2-PrOH content of the medium is too high, the $CHCl_3$ content of the core drops and the PS chains become kinetically frozen. As a result, the micelles remain as rigid spheres due to the vitrified PS core.

Nanorods vs Quantum Dots. In order to test the generality of the nanocrystal-induced micelle fusion and morphology transformation process, we carried out a small number of experiments with a sample of CdSe nanorods that happened to have the same band-edge absorbance maximum (555 nm) as the CdSe QDs described above. These nanorods had lengths of L_{rod} = 12 ± 2 nm and widths of 3 ± 0.3 nm.

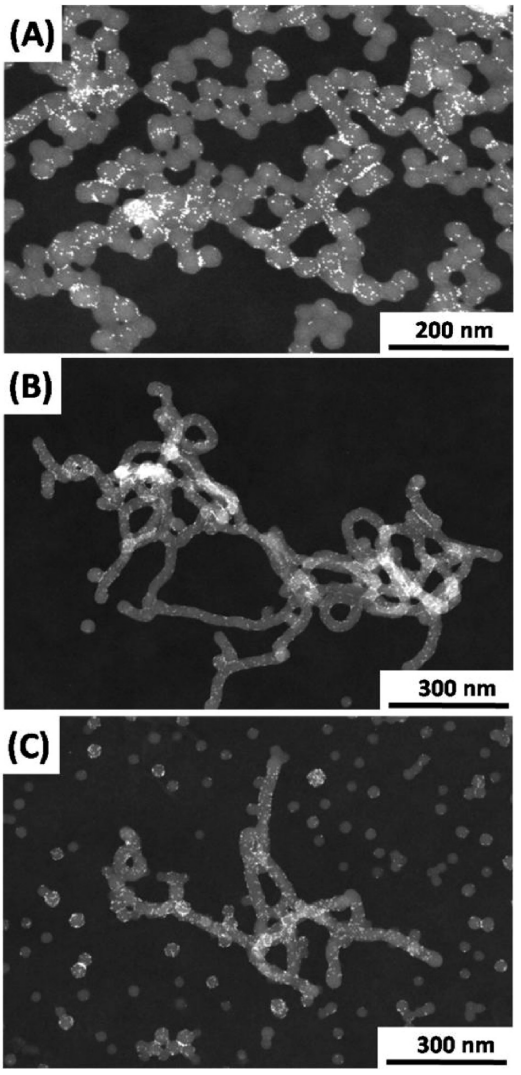

Figure 6. Dark-field TEM images of samples prepared from PS−P4VP + CdSe(555) stirred 50 h at 1250 rpm in various mixtures of $CHCl_3$/2-PrOH at ϕ_{2PrOH} = (A) 0.67, (B) 0.73, and (C) 0.77.

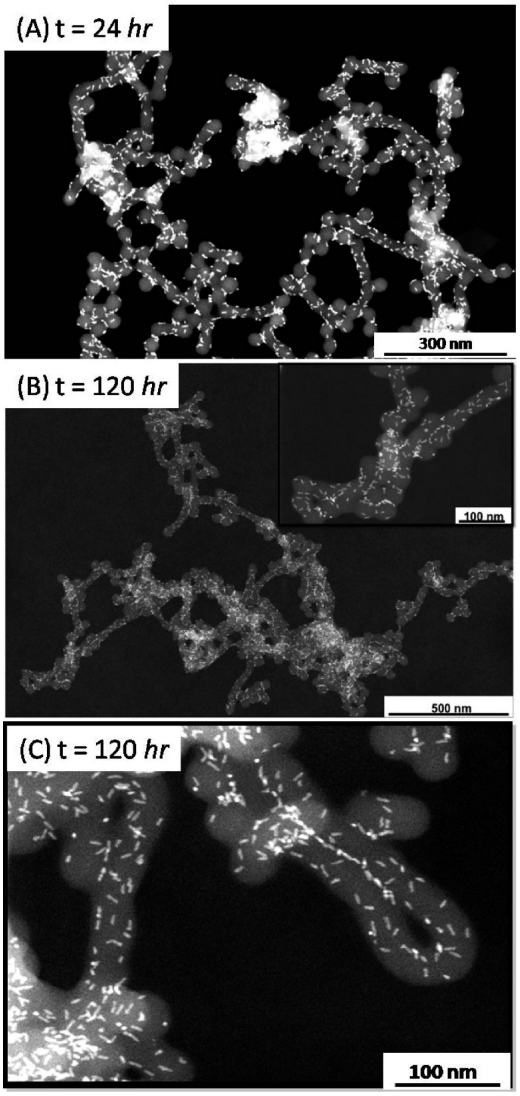

Figure 7. Dark-field TEM images of PS-*b*-P4VP/CdSe nanorods (L_{rod} = 12 ± 2 nm) in $CHCl_3$/2-PrOH ($\phi_{2\text{-PrOH}}$ = 0.73) stirred at 1250 rpm for (A) 24 h, (B) 120 h, and (C) 120 h.

Solutions were prepared in the same way and at the same polymer and nanocrystal concentration as for the CdSe(555) QDs in a chloroform−2-PrOH mixture with ϕ_{2PrOH} = 0.73. Images presented in Figure 7 demonstrate that the morphology transformation was slower in the presence of the nanorods than for the QDs. It was necessary to stir the solutions for 5 days to obtain networks consisting of uniform wormlike components. As one can see in Figure 7C, the nanorods tend to align along the long axis of the wormlike micelles, and there is also a tendency for them to be enriched where two wormlike micelles come into contact or at the junction of a wormlike micelle with a budding appendage.

Summary. We report a shear-induced transformation of spherical hybrid crew-cut micelles of PS_{404}−$P4VP_{76}$ diblock copolymer + CdSe quantum dots to wormlike networks. This transformation took place for a narrow range of $CHCl_3$ and 2-PrOH solvent mixtures in the range of $\phi_{2\text{-PrOH}}$ = 0.73. In the spherical micelles, the QDs were located in the P4VP corona of the micelles. We infer that this polymer acts as a multidentate ligand by coordination of pyridine units of the polymer to the surface sites of QDs. The morphology transition was induced by prolonged magnetic stirring solutions in 20 mL vials at 1250 rpm for 50 h. The networks consisted of wormlike micelles of uniform width in the form of loops and tails connected by T- and Y-branches. The width of the wormlike micelles was comparable to that of the diameter of the initial spherical micelles. Budding appendages to the wormlike micelles were wider and comparable in diameter to bulbous spherical caps at the ends of the dangling tails emanating from the networks. Dark-field TEM images show that within the collapsed networks on the grid, there was a strong tendency for the QDs to be concentrated at the contact surface between adjacent structures.

The main factors influencing the morphology transformation appear to be the presence of QDs in the micelles, solvent composition, and stirring speed. In the absence of QDs, some micelle aggregation to short wormlike structures could be detected by TEM. At slower stirring speeds (e.g., 250 rpm) aggregates with micrometer dimensions were formed, but many free QD-block copolymer hybrid micelles could be seen in the TEM images. At 1250 rpm, these free micelles were rare observations in the TEM images.

We explain this result qualitatively in terms of shear promoting collisions among the micelles, with the QDs in the corona forming bridges between adjacent micelles. These aggregates subsequently fused into wormlike micelles that in

turn formed loops and tails connected by T- and Y-branches. It is likely that the spherical hybrid micelles are favored kinetically in the mixed solvent with $\phi_{2\text{-PrOH}} = 0.73$, but that wormlike micelles or networks are favored thermodynamically due to solvent ($CHCl_3$) swelling of the micelle core. The formation of this type of network in mixed solvents has precedence in the work of Bhargava et al.[36,39] for a PS−PEO diblock copolymer in dimethylformamide−acetonitrile mixtures. How the micelle hybrids rearrange to networks within the aggregates in our system remains a mystery. The PS molecules within the micelle cores must be sufficiently mobile for micelle fusion to take place. Plasticization by $CHCl_3$ in the medium must be essential. Following ideas presented by Soos et al.,[38] we imagine that the highest shear rates within the stirred solution are responsible for the most significant morphology transformations. These include collisions between aggregates, perhaps promoting internal fusion, and shear degradation of the networks, limiting their size. The highest shear rates occur at the tip of the magnetic stirring bar.[37]

One of the unfortunate aspects of the vigorous stirring needed to carry out these morphology transformations is that the CdSe QDs are only weakly photoluminescent. This loss of photoluminescence efficiency is likely a consequence of surface oxidation. In future experiments, we plan to examine core−shell QDs and an oxygen-free atmosphere in an attempt to minimize the formation of surface traps. We also hope to develop a deeper understanding of the morphology transformation through the application of better defined shear fields.

Acknowledgment. The authors thank NSERC Canada for their financial support and Dr. M. Hines at Evident Technologies for providing us the CdSe QD samples.

Supporting Information Available: (1) CONTIN plots for PS_{404}−$P4VP_{76}$ micelles in the presence of CdSe(540) QDs or in the absence of QDs, in $CHCl_3$/2-PrOH ($\varphi_{2\text{-PrOH}} = 0.73$) at different stirring times; (2) TEM image of the supernate for a solution of CdSe(555)/PS_{404}−$P4VP_{76}$ hybrid micelles in $CHCl_3$/2-PrOH ($\varphi_{2\text{PrOH}} = 0.73$) aged 30 h without stirring; (3) TEM image of PS_{404}−$P4VP_{76}$ micelles in the absence of quantum dots in $CHCl_3$/2-PrOH ($\varphi_{2\text{-PrOH}} = 0.73$) after stirring for 5 min; (4) size distribution of the widths of wormlike structures and the diameters of buds and the end-caps; (5) turbidity as a function of stirring time for solutions of PS_{404}−$P4VP_{76}$/CdSe(540) hybrid micelles in $CHCl_3$/2-PrOH ($\varphi_{2\text{PrOH}} = 0.73$) stirred at 250 and 1250 rpm; (6) TEM images of CdSe(540)/PS_{404}−$P4VP_{76}$ mixture after 50 h stirring at 1250 rpm in different solvent compositions. This material is available free of charge via the Internet at http://pubs.acs.org.

References and Notes

(1) Riess, G. *Prog. Polym. Sci.* **2003**, *28*, 1107–1170.
(2) Astafieva, I.; Zhong, X. F.; Eisenberg, A. *Macromolecules* **1993**, *26*, 7339–7352.
(3) Zhang, L. F.; Eisenberg, A. *Science* **1995**, *268*, 1728–1731.
(4) Lin, E. K.; Gast, A. P. *Macromolecules* **1996**, *29*, 4432–4441.
(5) Discher, D. E.; Eisenberg, A. *Science* **2002**, *297*, 967–973.
(6) Discher, B. M.; Won, Y. Y.; Ege, D. S.; Lee, J. C. M.; Bates, F. S.; Discher, D. E.; Hammer, D. A. *Science* **1999**, *284*, 1143–1146.
(7) Won, Y. Y.; Davis, H. T.; Bates, F. S. *Science* **1999**, *283*, 960–963.
(8) Jain, S.; Bates, F. S. *Science* **2003**, *300*, 460–464.
(9) Liu, G. J.; Qiao, L. J.; Guo, A. *Macromolecules* **1996**, *29*, 5508–5510.
(10) Qian, J. S.; Zhang, M.; Manners, I.; Winnik, M. A. *Trends Biotechnol.* **2009**, *28*, 84–92.
(11) Hawker, C. J.; Russell, T. P. *MRS Bull.* **2005**, *30*, 952–966.
(12) Klingelhofer, S.; Heitz, W.; Greiner, A.; Oestreich, S.; Forster, S.; Antonietti, M. *J. Am. Chem. Soc.* **1997**, *119*, 10116–10120.
(13) Wang, H.; Wang, X. S.; Winnik, M. A.; Manners, I. *J. Am. Chem. Soc.* **2008**, *130*, 12921–12930.
(14) Dalhaimer, P.; Engler, A. J.; Parthasarathy, R.; Discher, D. E. *Biomacromolecules* **2004**, *5*, 1714–1719.
(15) Savic, R.; Luo, L. B.; Eisenberg, A.; Maysinger, D. *Science* **2003**, *300*, 615–618.
(16) Kwon, G. S.; Kataoka, K. *Adv. Drug Delivery Rev.* **1995**, *1*, 295–309.
(17) Torchilin, V. P. *J. Controlled Release* **2001**, *73*, 137–172.
(18) LaRue, I.; Adam, M.; Pitsikalis, M.; Hadjichristidis, N.; Rubinstein, M.; Sheiko, S. S. *Macromolecules* **2006**, *39*, 309–314.
(19) Chen, Q.; Zhao, H.; Ming, T.; Wang, J. F.; Wu, C. *J. Am. Chem. Soc.* **2009**, *131*, 16650–16651.
(20) Yu, H. Z.; Jiang, W. *Macromolecules* **2009**, *42*, 3399–3404.
(21) Bhargava, P.; Tu, Y.; Zheng, J. X.; Xiong, H.; Quirk, R. P.; Cheng, S. Z. D. *J. Am. Chem. Soc.* **2007**, *129*, 1113–1121.
(22) Cui, H. G.; Chen, Z. Y.; Zhong, S.; Wooley, K. L.; Pochan, D. J. *Science* **2007**, *317*, 647–650.
(23) Tessler, N.; Medvedev, V.; Kazes, M.; Kan, S. H.; Banin, U. *Science* **2002**, *295*, 1506–1508.
(24) Chan, W. C. W.; Nie, S. M. *Science* **1998**, *281*, 2016–2018.
(25) Huynh, W. U.; Dittmer, J. J.; Alivisatos, A. P. *Science* **2002**, *295*, 2425–2427.
(26) Alivisatos, A. P. *Science* **1996**, *271*, 933–937.
(27) Wang, M. F.; Kumar, S.; Lee, A.; Felorzabihi, N.; Shen, L.; Zhao, F.; Froimowicz, P.; Scholes, G. D.; Winnik, M. A. *J. Am. Chem. Soc.* **2008**, *130*, 9481–9491.
(28) Tang, Z. Y.; Kotov, N. A. *Adv. Mater.* **2005**, *17*, 951–962.
(29) Yu, W. W.; Qu, L.; Guo, W.; Peng, X. *Chem. Mater.* **2003**, *15*, 2854–2860.
(30) Wang, M. F.; Kumar, S.; Coombs, N.; Scholes, G. D.; Winnik, M. A. *Macromol. Chem. Phys.* **2010**, *211*, 393–403.
(31) Guerin, G.; Raez, J.; Manners, I.; Winnik, M. A. *Macromolecules* **2005**, *38*, 7819–7827.
(32) Provencher, S. W. *Comput. Phys. Commun.* **1982**, *27*, 213–227.
(33) Kuno, M.; Lee, J. K.; Dabbousi, B. O.; Mikulec, F. V.; Bawendi, M. G. *J. Chem. Phys.* **1997**, *106*, 9869–9882.
(34) Skaff, H.; Emrick, T. *Chem. Commun.* **2003**, 52–53.
(35) Jain, S.; Bates, F. S. *Macromolecules* **2004**, *37*, 1511–1523.
(36) Bhargava, P.; Zheng, J. X.; Quirk, R. P.; Cheng, S. Z. D. *J. Polym. Sci., Part B* **2006**, *44*, 3605–3611.
(37) Perez, J. A. S.; Porcel, E. M. R.; Lopez, J. L. C.; Sevilla, J. M. F.; Chisti, Y. *Chem. Eng. J.* **2006**, *124*, 1–5.
(38) Soos, M.; Moussa, A. S.; Ehrl, L.; Sefcik, J.; Wu, H.; Morbidelli, M. *J. Colloid Interface Sci.* **2008**, *319*, 577–589.
(39) Bhargava, P.; Zheng, J. X.; Li, P.; Quirk, R. P.; Harris, F. W.; Cheng, S. Z. D. *Macromolecules* **2006**, *39*, 4880–4888.